2021 43rd Annual International Conference of the
IEEE Engineering in Medicine & Biology Society (EMBC)
Oct 31 - Nov 4, 2021. Virtual Conference

Automatic Fall Protection for Hips Based on Micromechanical Double Gas Cylinder Rapid Puncture and Bionic Capsule Inflation

Yunkung Ning, Yanan Diao, Guanghui Wang, Nan Lou, Guanglin Li, *Senior Member, IEEE*, and Guoru Zhao*, *Member, IEEE*

***Abstract*—Wearable hip-protection airbags can effectively protect hip joints when elderly people fall. This has been studied all over the world, but similar products need to use special gas cylinders and replacement of new gas cylinders needs to return to the factory; The team previously designed a mechanical puncture protection system based on standard gas cylinders and standard threaded interfaces, but the airbag still has shortcomings such as the small protective area caused by a single gas cylinder. To solve the above problems, a set of wearable hip automatic protection systems based on micromechanical double gas cylinder rapid puncture (MDGCRP) is now designed. Through a large number of experiments, it was found that the response time of MDGCRP was 92ms and the execution time was 177.5ms. Compared with the single gas cylinder approach, the airbag provides greater protection to the hip while the filling time and module weight remain essentially unchanged. The system is triggered by physical and mechanical methods. Compared with chemical blasting or hot-melt methods, the system has the characteristics of low cost and consumables that can be safely and easily replaced by themselves.**

I. Introduction

According to statistics, about one-third of the elderly over the age of 65 have experienced falls every year, and about 10% to 15% of falls will cause serious injuries to the elderly and even death [1]. In addition to physical trauma, falls can also have a serious impact on the psychology of the elderly. About 75% of those who fall will have a fear of falling and are afraid to move again, which will further lead to the decline of the elderly's physical function [2]. According to the World Health Organization, the global cost of medical treatment due to fall injuries is more than 37 billion dollars, this medical cost is more than 5 billion RMB [3] in China.

In foreign countries, the wearable hip-protecting airbag inflation mechanism designed by researchers such as Chiba University of Japan [4-5] uses ignited gunpowder to melt through the gas cylinder, which has the advantage of filling the airbag within 120ms. The disadvantage is that gunpowder has a large Dangerous; American Active Protective Company designed an airbag that can be worn on the body and inflated the airbag through a cold air booster pump, effectively reducing 90% of the impact on the hip bone [6], Israel's Hip-Hope The belt device of this detection system, once it detects that it is about to hit the ground, the system immediately activates two fast-expanding airbags [7]. The above products need to be returned to the factory to replace the gas cylinder, which is not convenient for repeated use. Zhao's team of Shenzhen Institutes of Advanced Technology, Chinese Academy of Sciences have developed 5 generations of single gas cylinder puncture devices based on the link method [8] (SGCPDBOLM), cam method [9] (SGCPDBOCM), and hip protection capsule, which can deploy the airbag before a person falls to the ground. It is convenient to replace the gas cylinders but has the disadvantages that the airbag protection area is small and the gas volume is insufficient.

II. System Solution Design

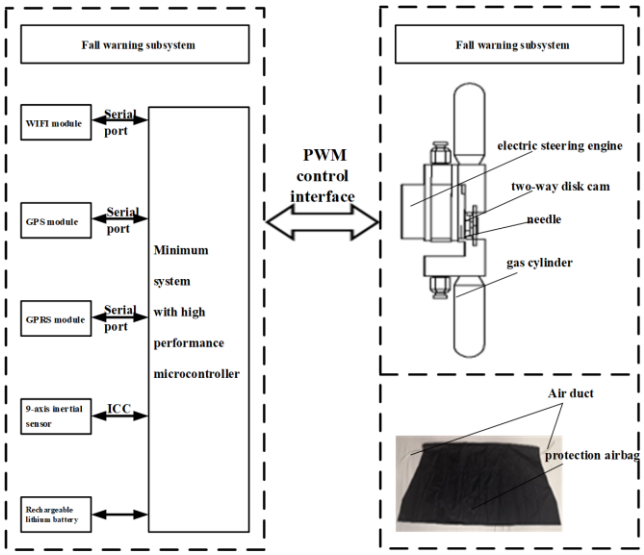

Figure 1 Block diagram of the wearable hip-protecting airbag system

The hip-protecting airbag system is shown in Figure 1. The 9-axis inertial sensor module is used to collect motion information. By extending Kalman filtering technology,

Yunkung Ning, Yanan Diao, Guanghui Wang, and Guanglin Li are with the CAS Key Laboratory of Human-Machine Intelligence-Synergy Systems, Research Center for Neural Engineering, Shenzhen Institutes of Advanced Technology, Chinese Academy of Sciences (e-mail: yk.ning@siat.ac.cn, yn.diao@siat.ac.cn, gh.wang@siat.ac.cn, gl.li@siat.ac.cn).

Nan Lou is with The University of Hong Kong-Shenzhen Hospital, Shenzhen, China. (e-mail: loun@hku-szh.org).

Guoru Zhao* is with the CAS Key Laboratory of Human-Machine Intelligence-Synergy Systems, Research Center for Neural Engineering, Shenzhen Institutes of Advanced Technology, Chinese Academy of Sciences (phone: +86-755-8639-2281; fax: +86-755-8639-2299; e-mail: gr.zhao@siat.ac.cn).

real-time motion posture monitoring can be achieved. The microcontroller can run machine-based motion monitoring and early warning Algorithm, when the system warns of a fall, it will trigger the dual-cylinder device to inflate the airbag and eject the capsule in the contracted state, thereby protecting the wearer's buffer before falling, and the system also uses GPS, WIFI, and base station triple positioning technology and low-power monitoring technology to achieve no blind area location tracking and long battery life monitoring. When a fall occurs, in addition to the voice real-time local alarm, the system can also transmit alarm and positioning information to remote monitoring centers and guardian's APPs via GPRS wireless network to take immediate action.

III. MECHANICAL PIERCING DEVICE

The electric steering engine is used to drive the bidirectional disc cam to rotate so that the disc cam pushes the driving ends of the pair of needling components, and the needling ends of the pair of needling components pierce a pair of gas cylinders respectively. MDGCRP can pierce two compressed gas cylinders at the same time, emitting twice as much gas as the original device. And the overall deflation time will not increase, a larger airbag can be designed to more effectively protect the hip joint when the elderly fall.

A. Piercing device design

The single gas cylinder piercing device is shown in Figure 2. The left link piercing device uses a steering engine to drive the steering gear rocker arm and a linear link to pierce the cylinder and release compressed gas [8]; The cam method piercing device uses a steering engine to drive the cam to push up the puncture needle to pierce the gas cylinder and realizes rapid automatic deflation [9].

As shown in Figures 4 and 5 is MDGCRP. The electric steering engine is an electric actuator that can convert electrical signals into rotating actions. The main role of the bidirectional disc cam is to transmit the torsional force of the steering engine to the two needles on both sides. The rotation of the steering engine was converted into the linear motion of the lancet. After theoretical calculations and multiple experiments, the optimal pressure angle and base circle radius of the disc cam was designed, so that the thrust of the lancet was enough to pierce the compressed gas cylinder, the fixed frame. The main function of the return spring is to allow the puncture needle to pop out quickly after piercing the gas cylinder, thereby ensuring that the gas cylinder can deflate quickly.

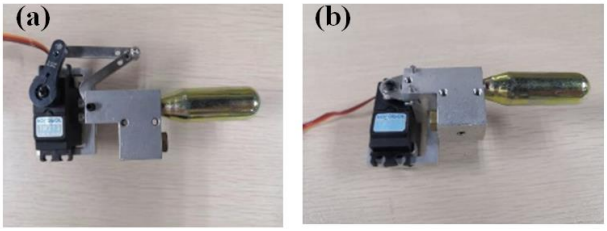

Figure 2 The single gas cylinder piercing device (a) SGCPDBOLM [8], (b) SGCPDBOCM [9]

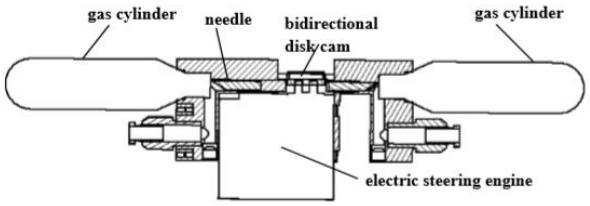

Figure 3 Schematic figure of MDGCRP

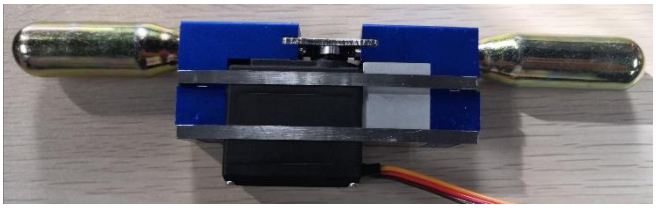

Figure 4 Physical figure of MDGCRP

The analysis of the force on the side of the bidirectional disc cam is shown in Figure 5. As the pressure angle increases, the effective component force gradually decreases, and the friction resistance gradually increases, which causes the cam mechanism to wear more easily. To some extent, it can also cause the cam mechanism to self-lock. Therefore, the smaller the pressure angle, the better the power transmission performance of the cam. Point A is the instantaneous coincidence point of cam and follower. According to the principle of relative motion, the pressure angle is calculated by Eq. 1.

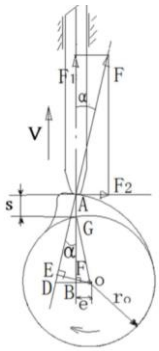

Figure 5 Force analysis of one side of bidirectional disc cam

$$\alpha = arctan\frac{\frac{ds}{d\varphi} - e}{s + \sqrt{r_0^2 - e_0^2}} \tag{1}$$

The output torque of the driving servo cannot be very large under the condition of low voltage, and the pressure angle range is preferably 15 ° ~ 25 °. According to the analysis of the effective force of the cam, the smaller the pressure angle, the greater the power of the transmission, but the premise of obtaining a small pressure angle is that the curvature of the cam contour curve is smaller, so the base circle and its contour area will increase, resulting in a cumbersome structure. Base circle radius is obtained by Eq. 2.

$$r_0 = \sqrt{(\frac{\frac{ds}{d\varphi} - e}{\tan\alpha} - s)^2 + e^2} \tag{2}$$

There is a contradiction between the radius of the base circle r_0 and the pressure angle α. To make the structure of the cam compact, the radius of the base circle should be as small as possible while satisfying $\alpha_{MAX} \le [\alpha]$. Where *e* is the eccentricity of the lancet, *s* is the stroke of the putter, *v* is the speed, α is the pressure angle, and r_0 is the radius of the cam base circle.

B. Structural Design of the airbag

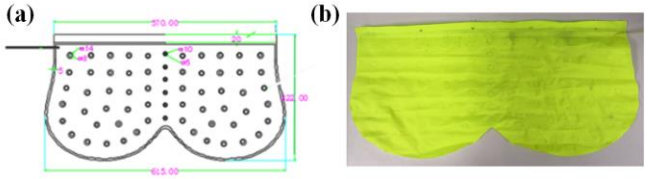

Figure 6 The former airbag (a) schematic diagram (b) physical figure

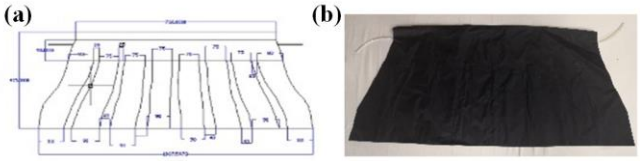

Figure 7 The current airbag (a) schematic diagram (b) physical figure

As shown in Figure 6, the former airbag is a single capsule structure made of TPU composite cloth. The outer layer of the cloth is a single-sided adhesive tape made of nylon fabric, and the inner layer is made of TPU film. The former airbag is 615mm long and 322mm wide, and it is about 22mm thick after being filled with gas. The gas is released through the venting pores. Now using MDGCRP, the airbag structure is shown in Figure 7. A strip-shaped structure made of nylon and TPU composite cloth is used. The airbag is about 1097mm long and 415mm wide. It is about 36mm thick, and the airbag is rapidly inflated at the same time through the two ends of the airbag. The increase in the length and width of the capsule can increase the area of protection for the elderly when they fall; the increase in the thickness of the full gas can absorb the impact of the ground on the human body after the fall; and the two ends are inflated at the same time, which can quickly fill the airbag and reduce the noise of the inflation process.

IV. Experimental Results and Analysis

Using a high-speed dynamic recorder to record the experimental process, the entire process of gas cylinder deflation can be divided into a response process and an execution process, where the response process is the time from the control circuit receiving the puncture command to the puncture needle just puncturing the gas cylinder; The execution process is the time when the gas is completely released after the puncture needle punctures the gas cylinder. The experiment was divided into 4 groups. SGCPDBOCM was used to deflate a 16g gas cylinder, a 12g gas cylinder, and an 8g compressed gas cylinder. MDGCRP of the same type of electric steering engine deflates two 8g compressed gas cylinders. Ten experiments were performed in each group and the average was taken. The results are shown in the table below.

TABLE I. Gas Release Schedule Of Different Specifications

specification	response time	execution time	total
One 12g	108.4	237.4	345.8
One 16g	109	284.5	393.5
One 8g	99.7	177.5	277.2
Two 8g	103.45	185.65	289.1

A. Response time result analysis

TABLE II. Response Time Normality Checklist For Cylinders Of Different Specifications

	Kolmogorov – Smirnov$^{\alpha}$			Shapiro-Wilk		
	Statistic	df	Sig.	Statistic	df	Sig.
Response	.116	40	.189	.958	40	.141

α.Lilliefors Significance Correction

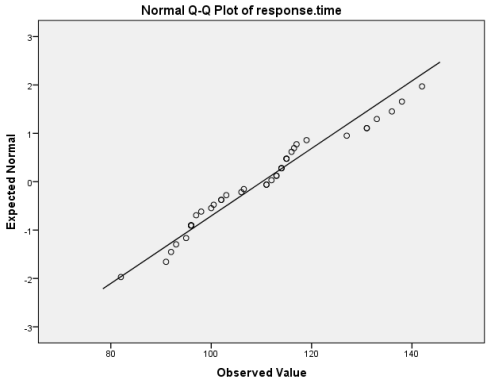

Figure 8 Q-Q chart of response time normality test of cylinders of different specifications

From Table 2 *Kolmogorov – Smirnov*$^{\alpha}$ normality test parameter Sig. = 0.189> 0.05; Figure 4 Q-Q diagram of response time normal test, the points are distributed near the straight line, which proves that the response time of gas cylinders of different specifications is normally distributed.

The response time of the four groups of experiments obeys a normal distribution $N(\mu_i, \sigma_0)$ equal to σ_0, and each group of experimental samples is independent of each other. The sample's mean of response time is X_i, the sample's standard deviations of response time are S_i, and the number of samples is n = 10; μ_i and σ_0 are unknown (i = 1,2,3,4). It is tested whether there is a difference between the average response time of the third and fourth groups. (α = 0.05). The test hypothesis is shown in Eqs. (3)-(5).

$$H_0 : \mu_3 - \mu_4 = 0, H_1 : \mu_3 - \mu_4 \neq 0 \tag{3}$$

$$S_w^2 = \frac{(n_3 - 1)S_3^2 + (n_4 - 1)S_4^2}{n_3 + n_4 - 2} = 76.84 \tag{4}$$

$$t = \frac{|x_3 - x_4|}{S_w\sqrt{\frac{1}{n_3} + \frac{1}{n_4}}} = 0.9566 < t_{\frac{\alpha}{2}}(n_3 + n_4 - 2) = 2.1009 \tag{5}$$

Therefore, it is not in the rejection domain, there are more than 95% of the reasons that the average response time of

piercing two 8g gas cylinders by MDGCRP is the same as the average response time of piercing an 8g compressed gas cylinder device by SGCPDBOCM. In the same way, it can be tested that the average response time of piercing two 8g gas cylinders by MDGCRP is not different from the average response time of SGCPDBOCM when deflating other compressed gas cylinders of different specifications

B. Analysis of execution time results

TABLE III. EXECUTION TIME NORMALITY CHECKLIST FOR PUNCTURING ONE 8G AND SIMULTANEOUSLY PUNCTURING TWO 8G CYLINDERS

	Kolmogorov – Smirnov$^{\alpha}$			Shapiro-Wilk		
	Statistic	df	Sig.	Statistic	df	Sig.
Execution	.178	20	.098	.960	20	.544

α.Lilliefors Significance Correction

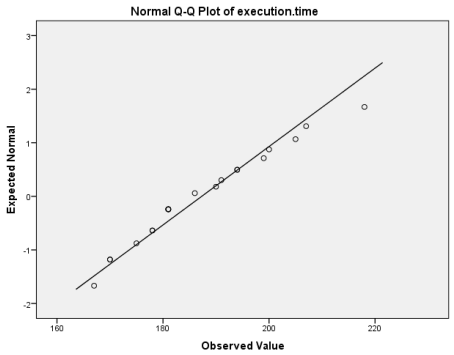

Figure 9 Execution time normality test for puncturing one 8g and two 8g gas cylinders at the same time Q-Q chart

From Table 3, *Kolmogorov – Smirnov*$^{\alpha}$ normality test parameter Sig. = 0.098> 0.05; Figure 5 Q-Q diagram of response time, the points are distributed near the straight line, it is proved that the execution time of puncturing one 8g and simultaneously puncturing two 8g gas cylinders is normally distributed.

The execution time of the two groups of experiments obeys a normal distribution $N(\mu_i,\sigma_0)$ equal to σ_0, and each group of experimental samples is independent of each other. The sample's mean execution time is X_i, the sample's standard deviations of execution time are S_i, and the number of samples n = 10; μ_i and σ_0 are unknown (i = 1,2,3,4). Check whether there is a gap between the average execution time of one 8g gas cylinder and two 8g gas cylinders (α = 0.05). The test hypothesis is shown in Eqs. (6)-(8).

$$H_0 : \mu_3=\mu_4, H_1 : \mu_3 < \mu_4 \tag{6}$$

$$S_w^2 = \frac{(n_3-1)S_3^2+(n_4-1)S_4^2}{n_3+n_4-2} = 81.37 \tag{7}$$

$$t = \frac{|x_3-x_4|}{S_w\sqrt{\frac{1}{n_3}+\frac{1}{n_4}}} = 0.9566 < t_\alpha(n_3+n_4-2) = 1.9341 \tag{8}$$

Therefore, it is not in the rejection domain, there are more than 95% of the reasons that the average execution time of piercing two 8g gas cylinders by MDGCRP is the same as the average execution time of piercing an 8g gas cylinder by SGCPDBOCM; However, piercing two 8g gas cylinders by using MDGCRP saves 26.5% time than piercing a 16g gas cylinder by SGCPDBOCM.

V. CONCLUSION

The simultaneous puncture of two 8g gas cylinders by MDGCRP, and SGCPDBOCM to deflate different specifications of gas cylinders, there is no difference in response time; however, piercing two 8g gas cylinders by using MDGCRP saves 104.4ms time than piercing a 16g gas cylinder by SGCPDBOCM. The protective airbags used twice the size of the former ones, providing more effective protection when the elderly fall, higher reliability, and less noise; triggered by physical and mechanical methods, gas cylinders can use standard threaded interfaces, so consumables are safer and more convenient than a chemical explosion or hot-melt methods.

ACKNOWLEDGMENT

The authors would like to thank all reviewers for their valuable comments. This study has been financed partially by the National Key R&D Program of China (2018YFC2001400/04, 2019YFB1311400/01), the Shenzhen Science and Technology Development Fund (JCYJ20170818163505850), the National Natural Science Foundation of China (61761166007, 71532014), Shandong Key R&D Program (2019JZZY011112), the Innovation Talent Fund of Guangdong Tezhi Plan (2019TQ05Z735), High Level-Hospital Program, Health Commission of Guangdong Province (HKUSZH201901023).

REFERENCES

[1] Loue S, Sajatovic M. Encyclopedia of Immigrant Health [J]. Springer Science Business Media, LLC.2012:671-672.

[2] Zhao G, Mei Z, Liang D, et al. Exploration and Implementation of a Pre-Impact Fall Recognition Method Based on an Inertial Body Sensor Network[J]. Sensors, 2012, 12(11):15338-15355.

[3] World Health Organization. Falls. [EB/OL]. [2017-12-25] http://www.who.int/mediacentre/factsheets/fs344/en/

[4] Tamura T, Yoshimura T, Sekine m, Uchida M, Tamura O. A wearable airbag to prevent fall injuries [J]. IEEE Transactions on Information Technology in Biomedicine, 2009(13): 910–914

[5] Yoshio Fukuda, Maria Q. Feng, James Zheng, and Virginia Halls. Rapid Detection of IED Light Emission Patterns for Activating a Head Protective System. IEEE SENSORS JOURNAL, 2016, 16(2).

[6] American Active Protective , KEEP YOURSELF UP TO DATE: OUR MOST RECENT NEWS. [EB/OL]. [2017-12-24]. https://activeprotective.com/

[7] Israel hit-hopt , Hip-Hope™ Smart Wearable Hip Protector Using Cutting-edge Technology and Design. [EB/OL]. [2017-12-25]. http://www.hip-hope.com/

[8] Mian Y., Qi Zz., Menghua L., et al. A Wearable Pre-impact Fall Early Warning and Protection System Based on MEMS Inertial Sensor and GPRS Communication[C].2015 IEEE 12th International Conference on Wearable and Implantable Body Sensor Networks (BSN), 2015.

[9] Huiqi Li, Yunkun Ning, Junfei Yang, Guoru Zhao. The Research of Wearable Fall Protective Airbag [J]. integrated technology , 2018,7(02):69-77